Heliyon 10 (2024) e32555

Contents lists available at ScienceDirect

Heliyon

journal homepage: www.cell.com/heliyon

Research article

Novel human recombinant N-acetylgalactosamine-6-sulfate sulfatase produced in a glyco-engineered *Escherichia coli* strain

Luisa N. Pimentel-Vera [a], Alexander Rodríguez-López [a,b], Angela J. Espejo-Mojica [a,b], Aura María Ramírez [a], Carolina Cardona [a,c], Luis H. Reyes [a,d], Shunji Tomatsu [e,f,g,h], Thapakorn Jaroentomeechai [i], Matthew P. DeLisa [i,j,k], Oscar F. Sánchez [l], Carlos J. Alméciga-Díaz [a,*]

[a] *Institute for the Study of Inborn Errors of Metabolism, Faculty of Science, Pontificia Universidad Javeriana, Bogotá, D.C., 110231, Colombia*
[b] *Dogma Biotech, Bogotá, D.C., 110111, Colombia*
[c] *Grupo de Investigaciones Biomédicas y de Genética Humana Aplicada GIBGA, Facultad de Ciencias de la Salud, Universidad de Ciencias Aplicadas y Ambientales U.D.C.A, Bogotá, D.C., Colombia*
[d] *Grupo de Diseño de Productos y Procesos (GDPP), Department of Chemical and Food Engineering, Universidad de los Andes, Bogotá, D.C., Colombia*
[e] *Nemours Children's Health, Wilmington, DE, 19803, USA*
[f] *Faculty of Arts and Sciences, University of Delaware, Newark, DE, 19716, USA*
[g] *Department of Pediatrics, Graduate School of Medicine, Gifu University, Gifu, 501-1193, Japan*
[h] *Department of Pediatrics, Thomas Jefferson University, Philadelphia, PA, 19144, USA*
[i] *Robert Frederick Smith School of Chemical and Biomolecular Engineering, Cornell University, Ithaca, NY, USA*
[j] *Nancy E. and Peter C. Meinig School of Biomedical Engineering, Cornell University, Ithaca, NY, USA*
[k] *Cornell Institute of Biotechnology, Cornell University, Ithaca, NY, USA*
[l] *Davidson School of Chemical Engineering, Purdue University, West Lafayette, IN, USA*

ARTICLE INFO

Keywords:
GALNS
Escherichia coli
N-linked glycosylation

ABSTRACT

Mucopolysaccharidosis IVA (MPS IVA) is a lysosomal storage disease caused by mutations in the gene encoding the lysosomal enzyme *N*-acetylgalactosamine-6-sulfate sulfatase (GALNS), resulting in the accumulation of keratan sulfate (KS) and chondroitin-6-sulfate (C6S). Previously, it was reported the production of an active human recombinant GALNS (rGALNS) in *E. coli* BL21(DE3). However, this recombinant enzyme was not taken up by HEK293 cells or MPS IVA skin fibroblasts. Here, we leveraged a glyco-engineered *E. coli* strain to produce a recombinant human GALNS bearing the eukaryotic trimannosyl core *N*-glycan, $Man_3GlcNAc_2$ (rGALNS*opt*Gly). The *N*-glycosylated GALNS was produced at 100 mL and 1.65 L scales, purified and characterized with respect to pH stability, enzyme kinetic parameters, cell uptake, and KS clearance. The results showed that the addition of trimannosyl core *N*-glycans enhanced both protein stability and substrate affinity. rGALNS*opt*Gly was capture through a mannose receptor-mediated process. This enzyme was delivered to the lysosome, where it reduced KS storage in human MPS IVA fibroblasts. This study demonstrates the potential of a glyco-engineered *E. coli* for producing a fully functional GALNS enzyme. It may offer an economic approach for the biosynthesis of a therapeutic glycoprotein that could prove useful for MPS IVA treatment. This strategy could be

* Corresponding author. Institute for the Study of Inborn Errors of Metabolism, Faculty of Sciences, Pontificia Universidad Javeriana, Cra 7 No. 43-82 Building 54, Room 305A. Bogotá, D.C., Colombia.
E-mail address: cjalmeciga@javeriana.edu.co (C.J. Alméciga-Díaz).

https://doi.org/10.1016/j.heliyon.2024.e32555
Received 19 February 2024; Received in revised form 14 May 2024; Accepted 5 June 2024
Available online 8 June 2024

extended to other lysosomal enzymes that rely on the presence of mannose N-glycans for cell uptake.

Abbreviations

anSME: Anaerobic sulfatase maturating enzyme
C6S: Chondroitin-6-sulfate
ConA: Concanavalin A
ERT: Enzyme replacement therapy
FGE: Formylglycine-generating enzyme
GAGs: Glycosaminoglycans
GALNS: *N*-acetylgalactosamine-6-sulfate sulfatase
GTase: Glycosyltransferase
KS: Keratan sulfate
di-KS: Di-sulfated KS
LSD: Lysosomal storage disease
MGM: Minimal growth medium
MPS IVA: Mucopolysaccharidosis IV A
MR: Mannose receptor
M6PR: Mannose-6-phsphate receptor
OTase: Oligosaccharyl transferase
rGALNS: Recombinant GALNS
rGALNS*opt*: Recombinant non-glycosylated human GALNS
rGALNS*opt*Gly: Recombinant *N*-glycosylated human GALNS

1. Introduction

Mucopolysaccharidosis IVA (MPS IVA, Morquio A syndrome, OMIM 253000) is a lysosomal storage disease (LSD) characterized by systemic skeletal dysplasia, laxity of joints, corneal clouding, hearing loss, valvular heart disease, and pulmonary complications [1]. MPS IVA is caused by mutations in the gene encoding the lysosomal enzyme N-acetylgalactosamine-6-sulfate sulfatase (GALNS, EC 3.1.6.4) that participates in the degradation of the glycosaminoglycans (GAGs) keratan sulfate (KS) and chondroitin-6-sulfate (C6S) [2]. Mutations in the GALNS gene lead to a loss or reduction of the enzyme activity, which results in the lysosomal accumulation of KS and C6S [2].

Enzyme replacement therapy (ERT) has been approved for Gaucher, Fabry, and Pompe diseases, late infantile neuronal ceroid lipofuscinosis type II, acid lipase deficiency, alpha-mannosidosis, and mucopolysaccharidoses (MPS) type I, II, IVA, VI, and VII [3,4]. For MPS IVA, the approved ERT is based on the infusion of the recombinant enzyme elosulfase alfa (Vimizim®) that is produced in Chinese Hamster Ovary (CHO) cells [5,6]. This enzyme has oligosaccharide chains with terminal mannose-6-phosphate (M6P) residues that allow cell uptake and lysosomal targeting via the M6P receptors (M6PRs) [7]. Although Elosulfase alfa is a therapeutic option for MPS IVA patients, current limitations include: (i) a limited effect on skeletal, corneal, and heart valvular issues; (ii) a short half-life of the enzyme and rapid clearance from circulation; (iii) a possible immunological response can be presented; and (iv) a high production cost [8,9].

An increasing number of studies have shown the possibility of producing active and therapeutic forms of lysosomal proteins in microorganisms [10–17]. This may enable the production of recombinant proteins with a reduced production cost, as well as improved stability, pharmacodynamics, and pharmacokinetic profiles [10,18]. *Escherichia coli* is one of the preferred hosts for producing recombinant proteins due to its easy manipulation, fast growth, and low culture cost [10,19–21]. Nevertheless, in *E. coli*, some of the posttranslational modifications observed in mammalian proteins, such as N-linked glycosylation, are not natively performed [19]. This is at odds with the growing demand for producing recombinant therapeutic proteins with human-like N-glycans since they are known to affect protein stability, solubility, therapeutic efficacy, immunogenicity, and half-life [22]. To address this shortcoming, different strategies have been described for the humanization of N-glycosylation pathways in microorganisms such as *E. coli*, *Saccharomyces cerevisiae*, and *Pichia pastoris* [18,23].

While *E. coli* cells do not natively perform protein glycosylation, pathways for N-glycosylation have been discovered in pathogenic bacteria, with the *Campylobacter* genus representing the most studied [23,24]. In *Campylobacter jejuni*, the *pgl* cluster encodes a general and bona fide N-glycosylation system [25]. Within this cluster, *pglB* encodes an oligosaccharyltransferase (OTase) that is an integral membrane protein sharing high identity with the catalytic subunit of the eukaryotic OTase STT3 [26,27]. PglB transfers a pre-assembled oligosaccharide molecule from a lipid-pyrophosphate donor to an asparagine residue in the acceptor protein. The N-glycosylation pathway of *C. jejuni* was functionally transferred to *E. coli*, enabling the production of N-glycosylated recombinant

proteins in this genetically tractable host [28]. Valderrama-Rincón et al. described the engineering of *E. coli* with a pathway for producing the eukaryotic trimannosyl core N-glycan (Man3GlcNAc2) and transferring this oligosaccharide to target proteins in the periplasm [29]. In this strain, the first step of the oligosaccharide synthesis involves the transfer of GlcNAc-1 phosphate to undecaprenyl phosphate by the glycosyltransferase (GTase) WecA. Subsequently, the oligosaccharide extension is mediated by the GTases Alg1, Alg2, Alg13, and Alg14 from *S. cerevisiae*, while the transfer of the oligosaccharide chain is performed by the *C. jejuni* PglB [30]. Expression of this artificial pathway allowed the production of recombinant proteins in *E. coli* that were site-specifically glycosylated with Man3GlcNac2 glycans, albeit with low yields initially [29] that were subsequently improved through metabolic pathway engineering [31].

Previously, we reported the production of an active human recombinant GALNS (rGALNS) in *E. coli* BL21(DE3) [32–35]. The purified enzyme exhibited similar pH, temperature, and serum stability profiles to those reported for rGALNS produced in CHO cells [33]. However, this recombinant enzyme was taken up neither by human embryonic kidney 293 (HEK293) cells nor MPS IVA skin fibroblasts [36]. These results suggest that N-glycosylation of GALNS is not necessary to produce active enzymes but appears to be crucial for cellular uptake. To address this shortcoming of non-glycosylated rGALNS, here we leveraged a glyco-engineered *E. coli* strain to produce rGALNS bearing N-linked Man3GlcNAc2 glycans (hereafter rGALNSoptGly). The results showed that rGALNSoptGly had higher stability and substrate affinity than its non-glycosylated counterpart. The N-glycosylated enzyme was also taken up by cultured cells and delivered to lysosomes, where it mediated the reduction of KS storage. Together, these results represent an essential step towards developing a novel ERT for MPS IVA, and possibly other LSDs, based on the use of glycoproteins produced in *E. coli* cells equipped with heterologous glycosylation machinery.

2. Materials and methods

Plasmids and strains. Human GALNS cDNA (GenBank accession number NM_000512.4) was codon-optimized for *E. coli* expression and synthesized by GeneArt® (Thermo Fisher Scientific, San Jose, CA, USA) [35]. Previously, it was reported that most rGALNS enzyme produced in *E. coli* BL21(DE3) was present as inclusion bodies [32]. To increase the amount of soluble protein, the GALNS cDNA sequence was optimized (rGALNS*opt*) by adapting the codon usage to the bias of *E. coli*, as well as by removing any negative *cis*-acting sites (*e.g.*, splice sites, TATA-boxes, etc.) [35]. The codon-optimized GALNS cDNA was inserted into the *Eco*RI and *Xho*I sites of the plasmid pGEX-5X-3 (GE Healthcare, Piscataway, NJ, USA) to produce pGEX-5X-GALNS*opt* (6.4 kb). To produce the *N*-glycosylated enzyme, we used the plasmid pYCG-PglB_{Cj} that encodes the *C. jejuni pglB* gene and *alg1, alg2, alg13,* and *alg14* genes from *S. cerevisiae* as well as *E. coli* strain MC4100 gmd*kan* Δ*waaL* [29]. This strain was engineered to promote a more efficient $Man_3GlcNAc_2$ biosynthesis through deletions in GDP-mannose dehydratase (GMD) and *waaL* genes, which increase the availability of GDP-mannose as a substrate for the N-glycosylation machinery [29]. To produce rGALNS*opt*Gly, the pGEX-5X-GALNS*opt* and pYCG-PglB_{Cj} plasmids were used to co-transform *E. coli* MC4100 gmd*kan* Δ*waaL* by electroporation. Since the *N*-glycosylation machinery, particularly *C. jejuni* PglB, operates on substrate proteins in the periplasmic space, secretion of rGALNS to the periplasm was expected to be essential for producing *N*-glycosylated enzyme. Hence, the native N-terminal signal peptide of GALNS was retained in the codon-optimized rGALNS*opt* gene sequence used here, since it has been demonstrated that this signal peptide allows secretion of rGALNS in *E. coli* [34,35].

Cells were grown in Luria-Bertani (LB) medium supplemented with ampicillin (100 μg/mL) and chloramphenicol (25 μg/mL). To produce the control enzyme lacking *N*-glycans (rGALNS*opt)*, the pGEX-5X-GALNS*opt* plasmid was used to transform *E. coli* BL21(DE3) and cultured in LB medium supplemented with ampicillin (100 μg/mL). The clones were selected by amplifying genes encoding GALNS and PglB from the plasmids using the primers GALNS*opt*_F 5′-CGATCATATGATGGCAGCAGTTGTTGC A-3′, GALNS*opt*_R 5′-CGATCTCGAGTT AATGTGACCACAGACA-3′, PglB*Cj*_F 5′-GGTGGTGGATCCCTGAAAAAAGAGTA-3′ and PglB*Cj*_R 5′-GGTGGTCGGCCGTTTTAAGTTTAAA-3’. All procedures were carried out using standard molecular biology methods [37].

Enzyme activity assay and protein quantification. GALNS activity was assayed using the substrate 4-methylumbelliferyl-β-D-galactopyranoside-6-sulfate (Toronto Chemicals Research, North York, ON, Canada) under previously described conditions [38]. One unit (U) was defined as the amount of enzyme needed to catalyze 1 nmol of substrate per hour. The GALNS activity was expressed as U mL^{-1} or U mg^{-1} of total protein. All proteins samples were quantified by Lowry assay.

Protein production at shake flask scale. *E. coli* MC4100 gmd*kan* Δ*waaL*/pYCG-PglB_{Cj} + pGEX-5X:GALNS*opt* and *E. coli* BL21 (DE3)/pGEX-5X:GALNS*opt* clones were cultured separately in 100 mL of modified minimal growth medium (MGM) [composition per liter: 20 g glucose, 13.23 g K_2HPO_4, 2.65 g KH_2PO_4, 2.04 g NaCl, 4.10 g $(NH_4)_2SO_4$, 0.5 g $MgSO_4{\cdot}7H_2O$, 0.026 g $FeCl_3$, 0.01 g thiamine, and 2.86 mL of trace-elements solution (0.022 g $AlCl_3$, 0.160 g $CoCl_6{\cdot}6H_2O$, 1.42 g $MnCl_2{\cdot}4H_2O$, 0.01 g $NiCl_2{\cdot}6H_2O$, 0.870 g $ZnSO_4{\cdot}7H_2O$, 1.44 g $CaCl_2{\cdot}2H_2O$, 0.023 g $Na_2MoO_4{\cdot}2H_2O$, 2.178 g $CuSO_4{\cdot}5H_2O$, and 0.010 g H_3BO_3), pH 7.2] [32] supplemented with the respective antibiotics. The cultures were carried out at 200 rpm and 37 °C for 24 h. After 8 h of culture, rGALNS production was induced with 1 mM IPTG (Invitrogen, Thermo Fisher Scientific, San Jose, CA, USA) [32], while the N-glycosylation machinery was induced with 0.2 % L-arabinose (Amresco, Solon, OH, USA) [29]. Negative control strains included *E. coli* MC4100 gmd*kan* Δ*waaL* co-transformed with empty pGEX-5X-3 and pYCG-PglB_{Cj} plasmids and *E. coli* BL21(DE3) with an empty pGEX-5X-3 plasmid. Samples of 1 mL were withdrawn at 0, 6, 12 and 24h post-induction to total protein and GALNS activity assays.

Bench-scale fermentation. Bench-scale production of rGALNS*opt* and rGALNS*opt*Gly was performed using a 3.7 L KFL2000 bioreactor (Bioengineering AG, Wald, Switzerland). Selected clones were cultured in 1.65 L of modified minimal growth medium (MGM), as described above [32], at 200 rpm for 24 h. At this scale, the effect of IPTG concentration (*i.e.*, 0.1 and 1 mM) and induction temperature (*i.e.*, 20 and 37 °C) on the enzyme production was tested. The production of rGALNS*opt* and rGALNS*opt*Gly was monitored for 24 h, and 20-mL aliquots were withdrawn at different times to measure total protein and GALNS activity.

Crude protein extraction and protein purification. After induction, the extracellular culture medium was harvested because active *N*-glycosylated rGALNS*opt*Gly was found within this fraction, due to the presence of the signal peptide of human GALNS. Total protein extract was obtained by centrifugation of the culture medium at 15,000×*g* for 30 min and sequential filtration through paper Whatman No. 1, and 0.45 μm and 0.22 μm polyether sulphone membranes (Durapore Membrane filters, EMD Millipore Corporation, Billerica, MA, USA). Cell-free culture medium was ultra-filtered through a 10-kDa cut-off membrane (EMD Millipore Corporation, Corporation, Billerica, MA, USA) to reach a final volume of 3 mL. The retentate was diafiltrated against equilibrium buffer (20 mM Tris-HCl, 500 mM NaCl, 1 mM $MgCl_2$, 1 mM $CaCl_2$; pH 7.4), and the enzyme was purified by affinity chromatography using a concanavalin A (ConA) Sepharose™ 4B column (GE Healthcare, Pittsburgh, PA, USA) in equilibrium buffer, and eluted with a linear gradient of 0–0.3 M of α-D-methyl-mannopyranoside (Sigma-Aldrich, St. Louis, MO, USA) in equilibrium buffer at a flow rate of 0.2 mL min^{-1} [29]. Fractions with the highest GALNS activity were pooled, diafiltrated against 25 mM sodium acetate pH 5.0, and stored at −80 °C for later use.

rGALNS*opt* was purified from the intracellular fraction since the highest GALNS activity was observed within this fraction. The cell lysate was obtained as previously described [32]. Briefly, the cell pellet was resuspended in 1 mL of lysis buffer (25 mM Tris, 1 mM phenylmethylsulphonyl fluoride, 1 mM EDTA, 5 % glycerol, 1 % Triton X-100, pH 7.2), sonicated 1 min at 4 °C and 25 % amplitude (Vibra-Cell, Sonics & Materials Inc., Newtown, CT, USA) and centrifuged at 2260×*g* and 4 °C for 15 min. The supernatant was diafiltrated against equilibrium buffer (25 mM sodium acetate, pH 5.0). rGALNS*opt* was purified by ion-exchange chromatography using a Macro-prep® High S-support column (Bio-rad, Hercules, CA, USA) in equilibrium buffer and eluted with a linear gradient of 0–0.5 M of NaCl in equilibrium buffer at a flow rate of 5 mL min^{-1} [14]. Fractions with the highest GALNS activity were pooled, diafiltrated against 25 mM sodium acetate pH 5.0, and stored at −80 °C for later use.

rGALNS was monitored in the pooled fractions by SDS-PAGE under reducing conditions (10 μg) and Western blot analysis using a polyclonal rabbit anti-GALNS IgG antibody produced against a mixture of highly immunogenic human GALNS peptides [14,34]. An anti-rabbit IgG coupled with peroxidase (Sigma-Aldrich, St. Louis, MO, USA) was used as the secondary antibody for visualization. Detection of *N*-glycans was performed using a horseradish peroxidase-conjugated Concanavalin A (ConA-HRP, EY Laboratories, Inc, San Mateo, CA, USA, Ref. H-1104-5) as described previously [29]. Briefly, after SDS-PAGE and protein transfer, the membrane was blocked with RIPA buffer (20 mM Tris-HCl, 150 mM NaCl, 0.1 % Triton-X100, 1 % sodium deoxycholate) for 1h. ConA-HRP was added to a final concentration of 0.3 μg/mL, in RIPA buffer and incubated for 2 h at room temperature (RT). The membrane was washed five times with RIPA buffer, and the assay was developed with 3,3′-diaminobenzidine solution (Sigma-Aldrich, St. Louis, MO, USA).

Enzyme characterization. The effect of pH on rGALNS*opt* and rGALNS*opt*Gly stability was evaluated between 3.2 and 7. For this, 10 μL of the purified enzyme were incubated with 10 μL of buffers at different pH (*i.e.*, 50 mM sodium citrate buffer pH 3.0 or pH 6.0, 50 mM acetate buffer pH 4.0 or pH 5.0, or 50 mM Tris–HCl buffer pH 7.0). Samples were incubated at 37 °C for 1 h [14,36], after which the enzyme activity was assessed as described above. All assays were performed in triplicate. Apparent kinetic parameters (K_M and V_{max}) for rGALNS*opt* and rGALNS*opt*Gly were estimated with 10 μg of recombinant protein and the 4-methylumbelliferyl-β-D-galactose-6-sulfate substrate at different concentrations (0, 0.5, 2, 5, 10, and 20 mM) under previously reported conditions [38]. K_M and V_{max} were calculated by fitting the experimental data to a Michaelis-Menten model using the GraphPad PRISM 6.0 software. As a control, kinetic parameters were also estimated for human GALNS from healthy human leukocytes. Blood samples (4–5 mL) were collected into heparin containing tubes. To separate the plasma layer from the red blood cells, dextran-heparin solution (1.6 mL, 3 %) was added to the whole blood tube and mixed thoroughly. After incubating for 1 h at room temperature, the upper plasma layer was carefully collected. The plasma was transferred to a clean tube, and an equal volume of cold distilled water was added to lyse the remaining red blood cells. After centrifugation at 2260×*g* for 3 min, the pellet of white blood cells was washed twice with cold distilled water. Subsequently, the pellet was resuspended in 400 μL of distilled water and lysed by sonication, twice, at 4 °C and 20 % amplitude for 10 s (Vibra-Cell, Sonics & Materials Inc., Newtown, CT, USA). All assays were performed in triplicate.

***In vitro* uptake and intracellular trafficking of GALNS enzymes.** Cellular uptake was evaluated in human skin fibroblasts derived from an MPS IVA patient. Fibroblasts from a healthy donor were used as controls. For this purpose, 1×10^5 cells per well were seeded in 6-well plates and cultured in Dulbecco modified Eagle medium (DMEM) supplemented with 2 mM L-glutamine, 15 % fetal bovine serum, 100 units of penicillin, and 100 g ml^{-1} of streptomycin, at 37 °C and 5 % CO_2. After 24 h, the culture medium was replaced with fresh medium 2 h before the addition the rGALNSoptGly to a final concentration of 50 nM, 100 nM, and 200 nM, and incubated for 24 h and 48 h at 37 °C and 5 % CO_2. To assess if the cellular uptake of rGALNS*opt*Gly was facilitated by mannose receptors, methyl α-D-mannopyranoside, a mannose receptor inhibitor, was added along with the enzyme. Specifically, confluent cells were exposed to concentrations of 100 and 200 nM of rGALNS*opt*Gly in the presence of 2 mM methyl α-D-mannopyranoside (Sigma-Aldrich St. Louis, MO, USA) and incubated for 24 h at 37 °C and 5 % CO_2 [39]. After cell incubation at different conditions, the culture medium was removed, and cells were washed with cold 1 × PBS (composition per liter: 8 g NaCl, 0.2 g KCl, 1.44 g NaH_2PO_4, 0.24 g KH_2PO_4, pH 7.2). Cells were then lysed by mixing with 1 % sodium deoxycholate (Sigma-Aldrich, St. Louis, MO, USA), and GALNS activity was assessed as described above. All the assays were performed in triplicate. Under approved protocols, experiments were carried out at Nemours Children's Health (Wilmington, DE, USA).

To evaluate intracellular trafficking, the rGALNS*opt*Gly enzyme was labeled with AlexaFluor 568® following the manufacturer's protocol (Molecular Probes, Thermo Fisher Scientific, San Jose, CA, USA). Then, HEK293 cells (CLR1573, ATCC, Manassas, VA, USA) were grown on coverslips treated with 0.01 % (w/v) type II collagen (Sigma-Aldrich, St. Louis, MO, USA) and plated onto 12-well plates. Cells were seeded at a density of 2×10^4 cells per well as described above. After 24 h, the culture medium was replaced with fresh medium 2 h before the addition of fluorescently labeled rGALNSoptGly at a final concentration of 50 nM. After 12 h of incubation with the labeled enzyme, the cells were stained with Lysotracker® Green DND-26 (Molecular Probes, Thermo Fisher Scientific, San Jose, CA, USA) following the manufacturer's protocol. Cells were then fixed using freshly prepared 4 %

paraformaldehyde in 1 × PBS for 20 min at RT, followed by 10 min of permeabilization with 0.2 % Triton X-100 in 1 × PBS. The cellular nucleus was stained with 4′,6-diamidino-2-phenylindole dihydrochloride (DAPI, Thermo Fisher Scientific, San Jose, CA, USA). Cells were imaged using an Olympus FV1000 confocal microscope equipped with 405, 473, and 559 nm laser lines using a 63 × /1.49 oil objective. DAPI (excitation 382–393, emission 417–477 nm), FITC (excitation 460–500 nm, emission 510–560 nm), and TRITC HyQ filter sets (excitation 530–560 nm, emission 590–650 nm) were applied to collect DAPI, Lysotracker® Green and Alexa 568 signals, respectively. Images were processed using NIH Image J software [40].

***In vitro* KS clearance assay.** MPS IVA skin fibroblasts (p.G116S) were obtained from a female patient with 7 years of age. The cells cultured and treated with 50 and 100 nM purified rGALNS*opt*Gly. Quantification of KS in the cell lysate was done by liquid chromatography coupled to a tandem mass spectrometry (LC-MS/MS) as previously described [41,42] with some modifications. Briefly, 200 µl of cell extract were placed into a 96-well Omega 10 K filter plate (AcroPrep™, PALL Corporation, NY, USA) and then centrifuged for 15 min at 2500×*g*. All samples and standards were incubated at 37 °C overnight with chondroitinase B, heparinase, and keratanase II (Seikagaku Co., Tokyo, Japan). After incubation, the disaccharides were collected by centrifugation for 15 min at 2500×*g* and analyzed by LC-MS/MS following a standardized protocol [42]. All assays were performed in triplicate. Experiments were carried out at Nemours Children's Health/Alfred I. duPont Hospital for Children (Wilmington, DE, USA) under approved protocols.

Statistical analysis. The results are shown as mean ± standard deviation (S.D.) and analyzed by ANOVA, followed by Šidák *t*-test. Differences between groups were considered significant when $p < 0.05$ on GraphPad PRISM 6.0.

3. Results and discussion

3.1. Production of recombinant N-glycosylated GALNS in engineered E. coli cells

Three co-transformed clones were randomly selected for culturing in 100 mL of MGM and analyzing rGALNS production. The selected clones exhibited a similar enzymatic activity profile during the induction (Fig. 1A and B). Notably, that the highest values activities of rGALNS*opt*Gly were found in the extracellular supernatant, with up to 0.19 U mg^{-1} and 0.24 U mL^{-1}, respectively. Importantly, these values were significantly above the background signals measured for the extracellular fraction derived from *E. coli* MC4100 gmd::*kan* Δ*waaL* co-transformed with empty pGEX-5X-3 and pYCG-PglB_{Cj} (0.02–0.05 U mg^{-1} and 0.03–0.05 U mL^{-1}) (Fig. 1A and B). On the other hand, in the intracellular fraction, the enzyme activity levels were about 0.03 U mg^{-1} and 0.09 U mL^{-1}, respectively, which were relatively low but still significantly above the intracellular fractions derived from the negative control strain, which gave undetectable signals (Fig. 1A and B).

Previous studies showed that the native signal peptide of GALNS could promote the accumulation of the enzyme in the extracellular supernatant under certain growth conditions [34], an observation that might explain the high extracellular rGALNS*opt*Gly activity levels observed here. Although N-terminal signal peptides such as the one present in rGALNS*opt* would not be expected to promote secretion beyond the periplasm, others have shown that periplasmic targeting of recombinant proteins in *E. coli* can result in

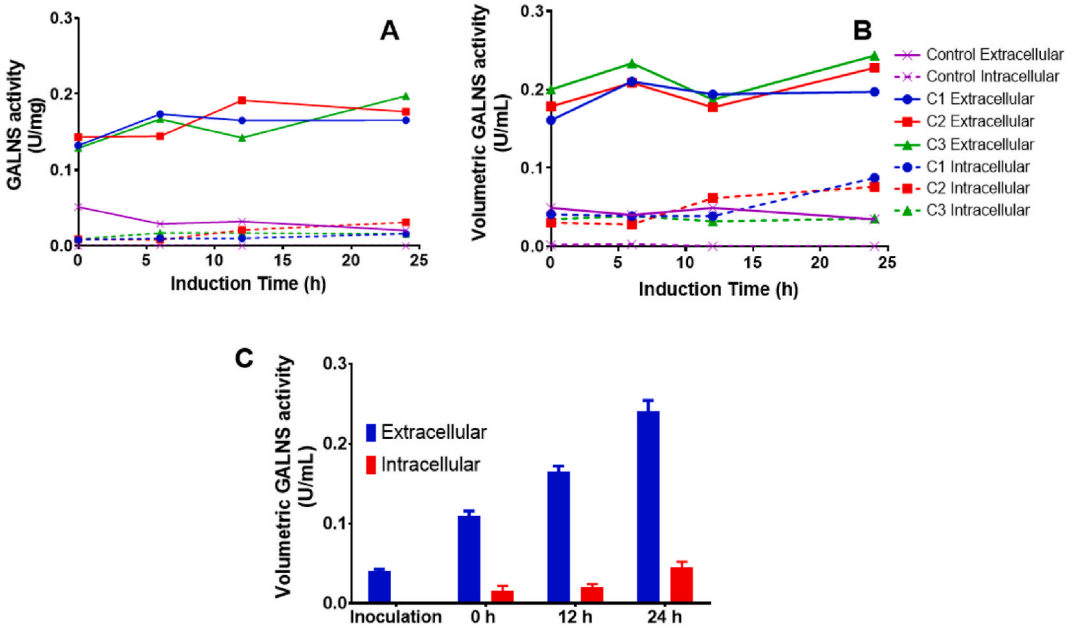

Fig. 1. Activity of rGALNS*opt*Gly produced from 100 mL of *E. coli* MC4100 gmd::*kan* Δ*waaL*. Normalized (A) and volumetric (B) GALNS activity from rGALNS*opt*Gly clones. Continuous lines represent extracellular activities while dashed lines represent intracellular activities. (C) GALNS activity without IPTG induction in the *E. coli* MC4100 gmd*kan* Δ*waaL*/pYCG-PglB_{Cj}/pGEX-5X:GALNS*opt*Gly strain.

unexpected secretion into the bacterial media without cell lysis [43]. We did not assay inclusion bodies for rGALNS activity since the *N*-glycosylated enzyme was not expected to be found in this fraction.

It is important to note that the enzyme activity of rGALNS*opt*Gly (0.19 U mg^{-1}) was lower than that reported for the rGALNS produced as a secreted protein in CHO cells, with activities between 120,000 and 170,000 U mg^{-1} [39,44]. This lower enzyme activity could be partially attributable to differences in the activation process of the enzyme. The Cys-to-FGly conversion in the active site of type I sulfatases is carried out before protein folding. Two different sets of enzymes mediate this process: (i) FGly-generating enzymes (FGEs) present in eukaryotes and aerobic prokaryotes; and (ii) the anaerobic sulfatase maturating enzymes (anSMEs) that have been described in some prokaryotes [45]. In mammals, FGE overexpression significantly increases the activity of sulfatases, favoring the production of enzymes with higher enzyme activity [14,46–49]. Our group shown that overexpression of *E. coli* AslB (an anSME-type enzyme) increased the activity of recombinant human sulfatase (i.e., GALNS and IDS) produced in *E. coli* by up to 4.6-fold [50]. The co-expression of AslB, together with the implementation of synthetic biology approaches [35] could be used in the future to improve the production and activity of the rGALNS produced in *E. coli*.

The detection of rGALNS activity at the beginning of the induction phase (Fig. 1A and B) suggests that rGALNS expression in *E. coli* MC4100 gmd*kan* Δ*waaL* was leaky, occurring prior to the addition of IPTG. To assess this leaky phenomenon, clones of co-transformed *E. coli* MC4100 gmd*kan* Δ*waaL* with pGEX-5X-GALNS*opt* and pYCG-$PglB_{Cj}$ were cultured in 100 mL of MGM without IPTG induction. Monitoring of rGALNS activity for these cultures showed the enzyme activity steadily increased from the time of inoculation in both the extra- and intracellular fractions (Fig. 1C). The highest volumetric rGALNS activity was observed in the extracellular fraction, showing activity similar to that obtained for the clones that were subjected to IPTG induction (Fig. 1B and C). The expression of rGALNS*opt* from plasmid pGEX-5X is under the control of the *tac* promoter, which is induced by IPTG. In addition, pGEX-5X carries a copy of $lacI^Q$, whose gene product represses the *tac* promoter and prevents the expression of the heterologous protein before induction. When pGEX-5X is used in *E. coli* BL21(DE3), the expression control is more stringent due to the presence of $lacI^Q$ in both the plasmid and the genome [51]. In contrast, *E. coli* MC4100 gmd*kan* Δ*waaL* has a large deletion in the lac operon [*F- araD139Δ(argF-lac)U169 rspL150 relA1 flbB5301 fruA25 deoC1 ptsF25*] [52] and lacks a genomic copy of $lacI^Q$, which could explain the leaky expression that we observed in this strain background. As mentioned before, little to no GALNS activity was detected in the fractions derived from the negative control, namely *E. coli* MC4100 gmd*kan* Δ*waaL* co-transformed with empty pGEX-5X and pYCG-$PglB_{Cj}$.

As has been reported extensively, a bottleneck in the production of recombinant proteins in *E. coli* relates to the formation of inclusion bodies [51,53]. In the production of active recombinant enzymes, the occurrence of inclusion bodies can be problematic because of the lack of correct protein folding [54]. In the case of rGALNS produced in *E. coli* BL21(DE3), previous studies have shown that the protein mainly accumulates as protein aggregates but with a lower enzyme activity than that observed in the intracellular soluble fraction [34,35]. Several strategies have been proposed to overcome this issue, such as the evaluation of culture conditions (*e.g.*, inducer concentration, cell density at the beginning of induction phase and culture temperature after induction), the use of physiologically regulated promoters, and the implementation of strategies to improve protein folding (*i.e.,* overexpression of native chaperones, enhancement of cytoplasmic disulfide bond formation, or fusion to a solubility enhancer such as maltose-binding protein) [34,35,51,53]. To promote correct folding and reduce the formation of inclusion bodies containing the recombinant protein, we assessed the effect of temperature during the induction phase and the concentration of the inducer on the activity of rGALNS. For these experiments, the production of recombinant enzymes was evaluated in scaled-up 1.65 L cultures induced with IPTG concentrations of 0.1 and 1.0 mM at induction temperatures of 20 °C and 37 °C. In the case of both rGALNS*opt* and rGALNS*opt*Gly, the highest specific activities in the intra and extracellular fractions were obtained with 0.1 mM of IPTG and 37 °C (Fig. 2A–D), and only low enzyme activities were observed in the inclusion bodies fraction derived from cultures expressing rGALNS*opt* (Fig. 2E). It should be noted that rGALNS*opt*Gly activity levels were lower than rGALNS*opt* regardless of the culture conditions, which was likely due to differences in

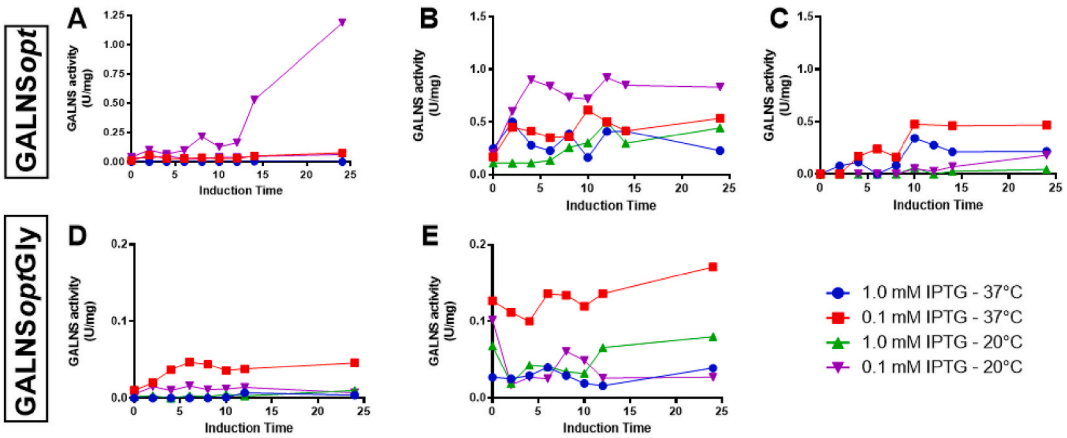

Fig. 2. Production of rGALNS at 1.65 L scale under different conditions. The rGALNS (A–C) and rGALNS*opt*Gly (D–E) enzymes were produced at 1.65 L under different IPTG concentrations (0.1 and 1 mM) and induction temperatures (20 and 37 °C). Enzyme activity was monitored in the intracellular (A, D), extracellular (B, E), and resuspended inclusion bodies (C) fractions.

the *E. coli* strains used for the production of each protein (*i.e.*, MC4100 gmd*kan* Δ*waaL* and BL21(DE3), respectively). Fig. 2 shows representative images of the enzyme activity profile under the different conditions evaluated, and similar results were obtained in replicate cultures (data not shown).

Characterization of rGALNS enzymes. SDS-PAGE of purified rGALNS*opt* and rGALNS*opt*Gly proteins showed the presence of bands between 35 and 66 kDa (Fig. 3A). Purified rGALNS*opt* and rGALNS*opt*Gly were analyzed by western and lectin blotting to verify the enzyme production and the presence of *N*-glycans, respectively (Fig. 3B and C). Under reducing conditions, prominent bands at ~30 kDa and weaker bands at ~50 kDa were recognized by the anti-GALNS antibody in the Western blot of rGALNS*opt* and rGALNS*opt*Gly (Fig. 3B). These results contrast with those reported by Rodriguez et al. [32], who produced a human recombinant GALNS in *E. coli*. Western blot analysis of this protein showed the presence of a ~50 kDa protein band in both the soluble and inclusion bodies fractions [32]. The difference in the Western blot between both studies may be related to the antibodies used. In Rodriguez et al., 2010, a monoclonal anti-GALNS antibody was used [32], whereas in the present study, an anti-GALNS IgG antibody raised against a mixture of highly immunogenic human GALNS peptides was used. In *P. pastoris*, this latter anti-GALNS antibody recognized bands of approximately 57 and 30 kDa [14]. It is noteworthy that additional bands were observed in rGALNS*opt*Gly, which were not detected in rGALNS*opt* and agrees with band profiles reported for GALNS enzymes purified from the liver [55], placenta [56], and recombinant CHO cells [44,57]. Based on the SDS-PAGE and western-blot results, we estimate a purity of >90 % for both recombinant

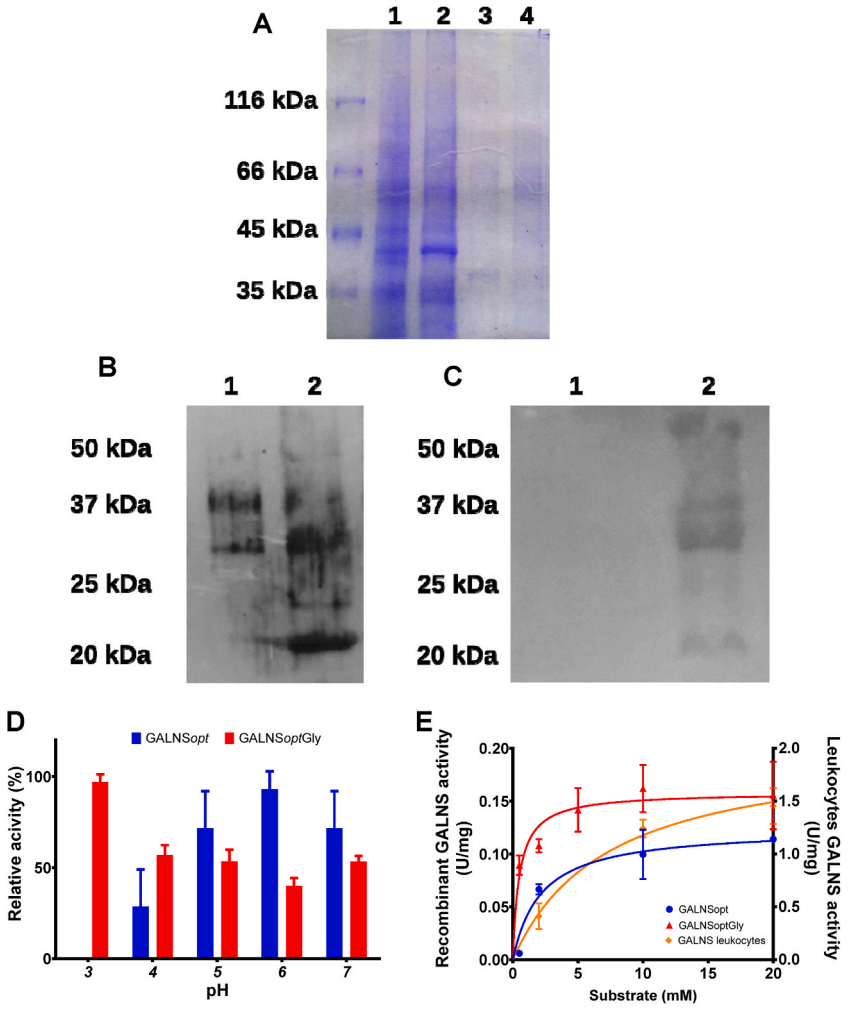

Fig. 3. Characterization of rGALNS and rGALNS*opt*Gly. (A) SDS-PAGE was performed on non-purified (lanes 1 and 2) and purified (lanes 3 and 4) rGALNSopt (lanes 1 and 3) and rGALNSoptGly (lanes 2 and 4). Western (B) and lectin (C) blot analysis were performed on purified rGALNS*opt* (lane 1) and rGALNS*opt*Gly (lane 2) proteins. rGALNS*opt* and rGALNS*opt*Gly were produced at 1.65 L under the best IPTG and temperature conditions identified for each protein. (D) pH stability of rGALNS*opt* and rGALNS*opt*Gly assayed by incubating each enzyme at pH 3.0, 4.0, 5.0, 6.0, and 7.0 for 1 h, after which GALNS activity was measured using the fluorogenic substrate. Activity values were normalized to the maximum enzyme activity at pH 6.0 and 3.0 for rGALNS*opt* and rGALNS*opt*Gly, respectively. No activity was detected at pH 3.0 for GALNS*opt*. (E) Michaelis-Menten enzyme kinetics of rGALNS*opt*, rGALNS*opt*Gly, and GALNS from human leukocytes. Data is the average of three biological replicates and error bars represent standard error of the mean.

proteins.

Glycosylation of rGALNS*opt*Gly produced in glyco-engineered *E. coli* was verified by cross-reaction of the enzyme with ConA (Fig. 3B), a lectin that is known to bind terminal α-mannose and was previously found to react with glycoproteins produced using this glyco-engineered *E. coli* strain [29]. As expected, rGALNS*opt* produced in *E. coli* BL21 (DE3) did not react with ConA (Fig. 3B). These results confirm the *E. coli*-based production of *N*-glycosylated rGALNS*opt*Gly bearing mannose terminal glycans and suggest that glycosylation might affect protein processing since new fragments were detected for rGALNS*opt*Gly but not rGALNS*opt* in Western blots. Importantly, human GALNS has two N-glycosylation sites, N204 and N423 [58,59] but only the N204 sequon (202-EANLT-206) contains a negatively charged residue in the −2 position, which is required for recognition by *C. jejuni* PglB to mediate oligosaccharide chain transfer [60]. Therefore, we speculate that rGALNS*opt*Gly produced in glyco-engineered *E. coli* is modified at N204. Previous studies with the glyco-engineered *E. coli* strain used here demonstrated glycosylation of recombinant proteins modified with an optimal DQNAT sequon preferen-tially recognized by *C. jejuni PglB* [29,31]. In this work, we took advantage of the fact that human GALNS has one native N-glycosylation sequon (202-EANLT-206) that coincides with the known acceptor-site specificity of *C. jejuni* PglB, which prefers an extended D-X_{-1}-N-X_{+1}-S/T motif [60]. Hence, these results are the first to show *N*-glycosylation of a native acceptor site using this glyco-engineered *E. coli* strain.

To evaluate the effect of N-glycosylation, the stability of both rGALNS*opt* and rGALNS*opt*Gly was evaluated by incubating each over a range of different pH values. The observed stability profiles for rGALNS*opt* and rGALNS*opt*Gly were notably different (Fig. 3D). rGALNS*opt* showed the highest stability at pH 6.0, which agreed with previous studies in which rGALNS produced in *E. coli* BL21(DE3) displayed its highest stability at pH 5.5 [36]. In addition, no statistically significant difference ($p < 0.05$) in the relative activity was observed between pH 5.0–7.0, and no enzyme activity was detected at pH 3.0 for rGALNS*opt*. In contrast, rGALNS*opt*Gly was much more stable under acidic conditions (*e.g.,* pH, 3.0), and as conditions became basic (*e.g.*, pH 4.0–7.0) the relative activity significantly decreased to below 50 %. This suggests that N-glycosylation directly affected the stability of rGALNS*opt*Gly, rendering it much more acid-resistant than its non-glycosylated counterpart. These results agree with previous findings that GALNS purified from the human placenta, which presumably carried *N*-glycans, was highly stable at pH values between 4.2 and 5.2 [61]. Overall, these observations are not entirely surprising given that N-glycosylation is well known to affect a range of different protein properties, such as folding, transport, signaling, and degradation [62], and has even been observed to play a significant role in stabilizing proteins at different pHs [62]. *In silico* simulations have shown that the surface area of the protein that is solvent-accessible decreases linearly as the number of *N*-glycans attached to the surface increases [63]. Thus, N-glycans effectively act as insulators between the protein and the solvent by increasing the molecular distance. This phenomenon helps prevent protein unfolding or denaturation by minimizing electrostatic interactions between the solvent and the protein.

We next evaluated the Michaelis-Menten apparent kinetic parameters of rGALNS*opt* and rGALNS*opt*Gly using 4-methyl-umbelliferyl-β-D-galactopyranoside-6-sulfate as substrate and lysate from human leukocytes as a positive control. The apparent K_M obtained here revealed that both rGALNS*opt* and rGALNS*opt*Gly have a higher affinity for the substrate than the GALNS enzyme in human leukocyte lysate (Fig. 3E and Table 1). The GALNS enzyme from human leukocyte lysate exhibited an apparent K_M value similar to that previously reported for fibroblasts, leukocytes, amniocytes, and chorionic villus [38,64]. rGALNS*opt*Gly exhibited the highest affinity, which was ~14- and ~4-fold stronger than the affinity observed for GALNS in human leukocyte lysate and rGALNS*opt*, respectively (Table 1). On the other hand, the V_{max} was similar between rGALNS*opt* and rGALNS*opt*Gly, as well as to that reported for GALNS from fibroblasts, leukocytes, amniocytes, and chorionic villus (Table 1) [38,64]. It is notable that the experimentally estimated V_{max} of GALNS from leukocyte lysate was higher than that previously reported for leukocytes and other cells (Table 1). In fact, the lysates used to estimate the GALNS V_{max} from fibroblasts, leukocytes, amniocytes, and chorionic villus were dialyzed [38,64]. This suggests the presence of molecules within the lysate that may affect GALNS activity. Nevertheless, these results show that presence of *N*-glycans' on the recombinant GALNS appears to affect the enzyme stability and the interaction with the substrate. However, the reasons for this increase in substrate affinity exhibited by the rGALNS*opt*Gly are unknown. We speculate that it might be related to differences in protein folding; however, further characterization of the ligand-protein interaction is needed to better understand this phenomenon.

Cellular uptake and intracellular trafficking. To determine if the *N*-glycans on rGALNS promote its internalization into mammalian cells, a cell capture assay was performed using human skin fibroblasts derived from an MPS IVA patient. We expected that the addition of $Man_3GlcNAc_2$ to GALNS would facilitate cellular uptake through the interaction between terminal mannose residues of the *N*-glycan and cell-surface mannose receptors (MRs), a mechanism that has been described for other lysosomal enzymes produced in

Table 1
Kinetic parameters reported for GALNS enzyme from different sources.

Source	K_M (mM)[a]	V_{max} (U/mg)	R^2	Ref
rGALNS*opt*	2.16 ± 0.10	0.125 ± 0.016	0.88	This study
rGALNS*opt*Gly	0.50 ± 0.19	0.158 ± 0.010	0.67	This study
Leukocytes	7.28 ± 2.21	2.034 ± 0.232	0.97	This study
Fibroblast	7.77	0.106	–	[38]
Leukocytes	7.77	0.189	–	[38]
Amniocytes	7.0	0.141	–	[64]
Chorionic Villus	7.0	0.088	–	[64]

Note: error is reported as ± standard error of the mean ($n = 3$).
[a] The substrate used was 4-methylumbelliferyl-β-D-galactopyranoside-6-sulfate.

different expression hosts such as moss, carrot cells, rice and *P. pastoris*, all of which attach mannose-terminal *N*-glycans on their glycoproteins [10,12,14,18,65–67]. We previously demonstrated that rGALNS produced in *E. coli* is not taken up by cultured HEK293 cells or MPS IVA fibroblasts [36]. Based on this previous observation, cell capture and intracellular traffic assays were only performed for rGALNS*opt*Gly.

The intracellular activity of GALNS was measured in MPS IVA fibroblasts treated with different concentrations of rGALNS*opt*Gly after 24 and 48 h. After 24 h of rGALNS*opt*Gly treatment, the intracellular activity of the enzyme was significantly greater ($p < 0.01$) than the activity measured in the negative control or untreated MPS IVA fibroblasts (Fig. 4A). However, almost constant enzyme activity was observed despite the different rGALNS*opt*Gly concentrations. The lack of concentration dependence for the enzyme activity suggested that MRs were saturated under the conditions tested, which seems likely given the low expression of MRs in human skin fibroblasts [67,68]. The recombinant enzyme activity was between 2 and 4-fold higher than that observed in control fibroblasts ($p < 0.05$). After 48 h of rGALNS*opt*Gly treatment, a significant drop in the enzyme activity was observed in the MPS IVA fibroblasts. The enzyme activity in the fibroblasts treated with 100 and 200 nM rGALNS*opt*Gly was still higher than in untreated fibroblasts ($p < 0.05$); however, these activities were about 50 % of the activity observed control fibroblasts ($p < 0.05$). When 50 nM of the recombinant enzyme was used, no activity was detected after 48 h of treatment. We suspect that cellular processes may have promoted rapid clearance of the enzyme at this concentration and that concentrations as high as 100 nM of rGALNS*opt*Gly may be needed to achieve residual activity inside cells.

To assess the cellular internalization of the recombinant enzyme via MRs, we performed an inhibition capture assay using the MR inhibitor methyl-alpha-D-mannopyranoside. We chose to use concentrations of 100 and 200 nM of rGALNS*opt*Gly and a 24-h incubation time because of the relatively large enzyme activity observed under these conditions. Adding the MR inhibitor to the system decreased the activity of rGALNS*opt*Gly to a level that was comparable to the negative control or untreated MPS IVA fibroblasts (Fig. 4B), indicating that rGALNS*opt*Gly is taken up through cell-surface MRs. Importantly, these results show for the first time that the eukaryotic $Man_3GlcNAc_2$ *N*-glycan synthesized by glyco-engineered *E. coli* cells can mediate the uptake of a recombinant protein. Our observations agree with previous reports of lysosomal enzymes produced in hosts that synthesize *N*-glycans with terminal mannoses, such as α-galactosidase A (*P. pastoris*, [69]), lysosomal acid lipase (*P. pastoris*, [11,12]), iduronate-2-sulfate sulfatase (*P. pastoris*, [13]), GALNS (*P. pastoris*, [14,15]), (*P. pastoris*, β-hexosaminidases [16,17]), glucocerebrosidase (carrot cells, [66]), and acid α-glucosidase (rice, [65]). Nevertheless, it is important to highlight that proteins produced in these hosts have about 8–12 mannose residues [12,18,

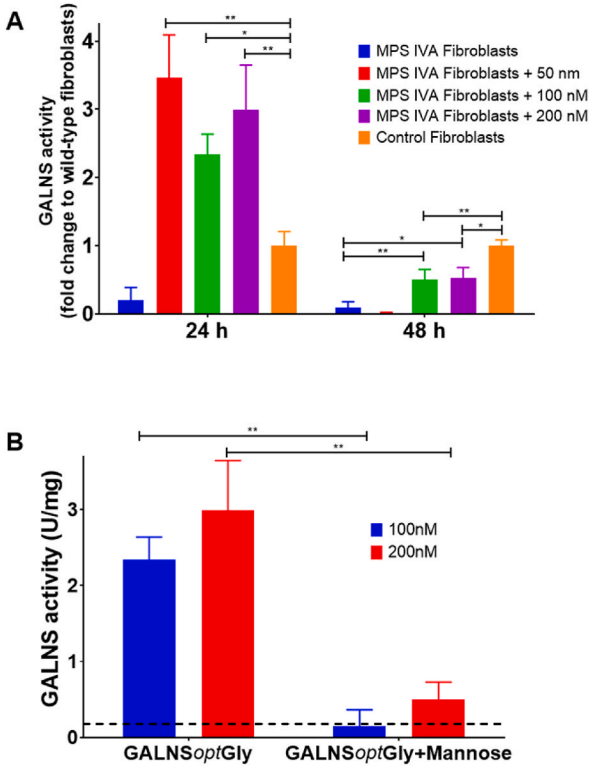

Fig. 4. Cellular uptake assay. (A) Cellular uptake of rGALNS*opt*Gly assayed in cultured MPS IVA fibroblasts with 50, 100 and 200 nM of the enzyme. Fibroblasts from a healthy donor were used as control. The enzyme activity was assayed in the cell lysate after 24 and 48 h of treatment. (B) rGALNS*opt*Gly was added to MPS IVA fibroblasts with or without a mannose receptor inhibitor (methyl-alpha-D-mannopyranoside). The enzyme activity was assayed in the cell lysate after 24 h of treatment. The dashed line represents the activity of MPS IVA fibroblasts treated with PBS. Data is the average of three biological replicates and error bars represent standard error of the mean. *$p < 0.05$, **$p < 0.01$.

65,70] whereas the glyco-engineered *E. coli* strain used here synthesizes a simpler trimannosyl *N*-glycan [29], which appears to be sufficient for promoting protein uptake.

To visualize the cellular internalization of the recombinant enzyme and determine whether it co-localized with lysosomes, rGALNS*opt*Gly was labeled with AlexaFluor 568® and incubated for 12 h with HEK293 cells at a concentration of 50 nM. After lysosome and nuclei staining, the cells were visualized by confocal microscopy (Fig. 5A–C). Tracking of fluorescently labeled rGALNS*opt*Gly revealed that the enzyme was internalized into the cells and co-localized with lysosomes. Representative images of two different zones showed clear co-localization of rGALNS*opt*Gly with lysosomes (Fig. 5D and E, yellow spots). Similar results were observed in a duplicate assay performed under the same conditions (data not shown), confirming the reproducibility of rGALNS*opt*Gly internalization and its co-localization with lysosomes. The overlap of these signals was confirmed by a 3D surface plot analysis, in which it was possible to observe co-localization events between lysosomes (green) and enzyme (red) (Fig. 5F and G). A significant fraction of the enzyme appears in other non-acidic cell compartments, such as the endosomal pathway. Similar results were observed for a recombinant GALNS produced in CHO cells that was tested in human MPS IVA chondrocytes [44].

It is important to note that targeting MRs and mannose-6-phosphate receptors (M6PRs) is not the only cell mechanism to capture lysosomal proteins. Other receptors that can participate in this process have been described. For instance, the Endo180 receptor, part of the MR family and found in HEK293T cells and fibroblasts, plays a vital role in the intracellular collagen degradation pathway through lysosomes [68,71]. Endo180 and MRs share two domains, one is the FNII domain that recognizes collagen, and the other is the lectin activity domain (CTLD2 in Endo 180 or CLTD4 in MR) that binds mannose, fucose, and GlcNAc in a Ca^{2+}-dependent manner [72, 73]. It has also been reported that certain lysosomal enzymes, *e.g.*, non-phosphorylated cathepsin D and B, were transported to lysosomes without of the M6PR instead of using the LDL receptor and LDL receptor-related protein 1 (Lrp1) [74]. Therefore, it is possible that other receptors besides (or in addition to) MRs mediate the cellular uptake and lysosomal delivery of rGALNS*opt*Gly in HEK293 cells and MPS IVA fibroblasts.

KS clearance. Finally, to test the therapeutic potential of rGALNS*opt*Gly, we measured the depletion of di-sulfated KS (di-KS) by LC-MS/MS after the treatment of MPS IVA fibroblasts with the recombinant enzyme. GALNS removes the sulfate group from C(6) D-galactose from de di-KS [Gal(6S)β1 → 4GlcNAc(6S)] producing mono-sulfated KS [Galβ1 → 4GlcNAc(6S)] [75]. In this sense, a decrease in GALNS activity may result in an increase in di-KS. Quantification of di-KS by LC-MS/MS showed a more significant difference between MPS IVA patients and age-matched controls than mono-sulfated KS, proposing it as a novel biomarker for MPS IVA [75].

Treatment of MPS IVA fibroblasts with 50 and 100 nM of rGALNS*opt*Gly for 24 h resulted in a significant reduction ($p < 0.01$) of intracellular di-KS (Fig. 6). There was no significant difference observed between cells treated with 50 and 100 nM of the enzyme, similar to our cellular uptake assays and indicative of fibroblast MR saturation at these concentrations of rGALNS*opt*Gly. After 48 h of treatment with 50 and 100 nM of rGALNS*opt*Gly, the di-KS concentrations returned to the level observed in untreated MPS IVA fibroblasts, which agreed with the results above showing that intracellular GALNS activity in MPS IVA fibroblasts dropped after 48 h of enzyme treatment. Despite the observed cellular clearance of rGALNS*opt*Gly over more extended periods, this is the first time that a recombinant lysosomal enzyme produced in *E. coli* was able to catalyze the reduction of storage material, showing the potential of this

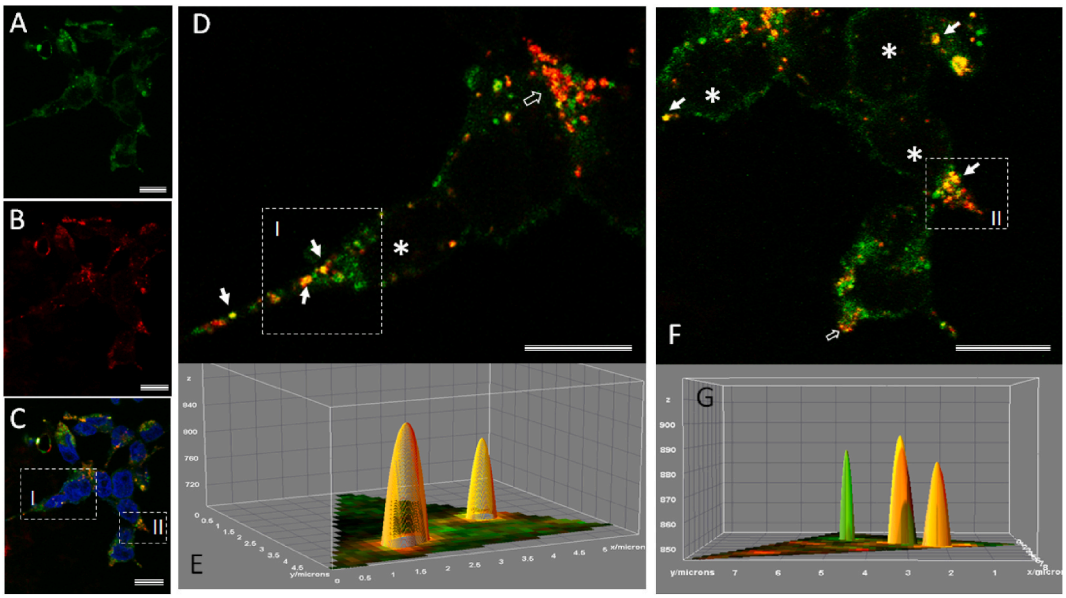

Fig. 5. ***In vitro*** **cell co-localization assay.** (A) Lysotracker labeling of lysosomes. (B) AlexaFluor 568® labeled rGALNS*opt*Gly. (C) Merged image (nuclei were stained with DAPI). Magnified segment I from panel C (D) and segment II from panel C (E). 3D surface plot from the delimited region in panel D (F) and panel E (G). Open arrows indicate rGALNS*opt*Gly that was detected within the cell, white arrows indicate rGALNS*opt*Gly-lysosome co-localization, and asterisks indicate nuclei. Scale bar: 13 μm.

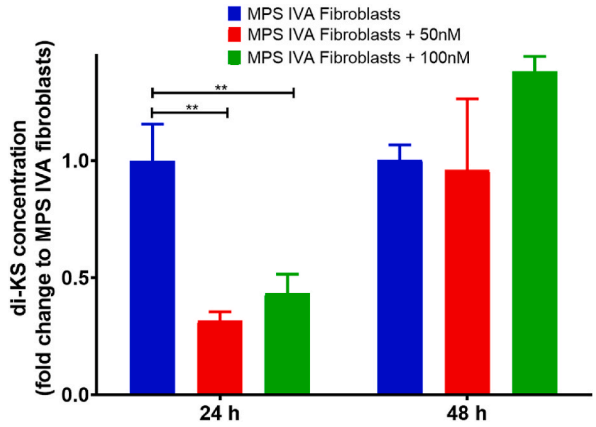

Fig. 6. Keratan sulfate clearance in MPS IVA fibroblasts. Di-keratan sulfate (di-KS) levels were determined in intracellular extracts of MPS IVA fibroblasts after 24 h (A) and 48 h (B) treatment with 50 and 100 nM rGALNS*opt*Gly. The di-KS concentration was normalized to the concentration in MPS IVA fibroblasts. $^{**}p < 0.01$.

approach for the development of an ERT for MPS IVA syndrome, as well as for other lysosomal storage diseases. It is also important to consider that skin fibroblasts might not represent the best cellular model for MPS IVA since no skin problems have been reported in MPS IVA patients [76]. Thus, future studies should investigate other cell types, such as chondrocytes and cardiomyocytes, as models for evaluating this recombinant enzyme, as well as the use of MPS IVA animal models [77–79]. Such studies have been described by Dvorak-Ewell et al., who showed an 80–100 % reduction in KS levels in human MPS IVA chondrocytes treated for six weeks with 1 nM or 10 nM of a recombinant GALNS produced in CHO cells [44]. Notably, the LC-MS/MS methodology used to quantitate oligosaccharides derived from KS has previously been used only in human fluids such as blood, cerebral spinal fluid, and urine [41,42,80]. The results presented here represent the first time that this methodology has been used to quantify KS-derived oligosaccharides from cultured cells, representing a significant advance that might pave the way for high-throughput screening programs to identify new treatment alternatives for MPS IVA [81].

In conclusion, we have demonstrated, through different ways, the production of a recombinant *N*-glycosylated human GALNS enzyme using a glyco-engineered *E. coli* strain. Evidence for $Man_3GlcNAc_2$ glycosylation was three-fold: (1) rGALNS*opt*Gly was purified by affinity chromatography using a ConA column; (2) lectin-blot using ConA-HRP showed that only rGALNS*opt*Gly but not rGALNS*opt* was recognized; and (3) rGALNS*opt*Gly was internalized by human skin fibroblasts, and this uptake was completely blocked in the presence of the MR inhibitor methyl-alpha-D-mannopyranoside. The results establish that the addition of eukaryotic trimannosyl core *N*-glycans may enhance rGALNS protein stability and enzyme-substrate affinity. In addition, the N-glycan containing mannose facilitated cellular uptake through a receptor-mediated process, resulting in intracellular enzyme activity levels that were comparable to or even higher than those observed in wild-type cells. This protein was delivered to lysosomes, catalyzing the reduction of stored KS material. This study represents the first report of a lysosomal enzyme produced in a glyco-engineered *E. coli* strain. It reveals the potential of this system for producing recombinant lysosomal enzymes that rely on the presence of mannose N-glycans for cell uptake. However, the enzyme activity of rGALNS*opt*Gly was significantly lower than that reported for recombinant GALNS produced in mammalian cells. This may limit the translation of this enzyme to the clinics. Future studies should focus on increasing the rGALNS*opt*Gly activity through strategies such as co-expression of *E. coli* sulfatase maturing enzyme AslB, implementing synthetic biology approaches, and regulating the cellular stress response [35,50]. Additionally, other N-glycans should also be taken into consideration, including those with mannose-6-phosphate ends.

Ethics statement

The project was approved by the Research and Ethics Committee of the Faculty of Science of the Pontificia Universidad Javeriana (Minute 6, May 18, 2012). *In vitro* experiments were also carried out at Nemours Children's Health (Wilmington, DE, USA) under approved protocols.

CRediT authorship contribution statement

Luisa N. Pimentel-Vera: Writing – review & editing, Writing – original draft, Methodology, Investigation, Formal analysis. **Alexander Rodríguez-López:** Writing – review & editing, Writing – original draft, Methodology, Investigation, Formal analysis. **Angela J. Espejo-Mojica:** Writing – review & editing, Writing – original draft, Formal analysis. **Aura María Ramírez:** Writing – original draft, Investigation. **Carolina Cardona:** Writing – review & editing, Writing – original draft, Formal analysis. **Luis H. Reyes:** Writing – review & editing, Writing – original draft, Formal analysis. **Shunji Tomatsu:** Writing – review & editing, Writing – original draft, Formal analysis. **Thapakorn Jaroentomeechai:** Writing – original draft, Formal analysis. **Matthew P. DeLisa:** Writing – review & editing, Writing – original draft, Conceptualization. **Oscar F. Sánchez:** Writing – review & editing, Writing – original draft,

Conceptualization. **Carlos J. Alméciga-Díaz:** Writing – review & editing, Writing – original draft, Supervision, Project administration, Funding acquisition, Conceptualization.

Declaration of competing interest

The authors declare that they have no known competing financial interests or personal relationships that could have appeared to influence the work reported in this paper.

Acknowledgements

ARL received a doctoral scholarship from Pontificia Universidad Javeriana. AEM and OFS received a doctoral scholarship from the Ministerio de Ciencia, Tecnología e Innovación (MinCiencias). CC and LHR were supported by "Es Tiempo de Volver" initiative from MinCiencias. CJAD was supported by Pontificia Universidad Javeriana [InvestigarPUJ 20567 and 20646] and MinCiencias [Grant ID 5174 - contract No. 120356933205, and Grant ID 5170 - contract No. 120356933427].

References

[1] K. Sawamoto, et al., Mucopolysaccharidosis IVA: diagnosis, treatment, and management, Int. J. Mol. Sci. 21 (4) (2020).
[2] K. Sawamoto, et al., Mucopolysaccharidosis type IVA: clinical features, biochemistry, diagnosis, genetics, and treatment, in: S. Tomatsu, et al. (Eds.), Mucopolysaccharidoses Update (2 Volume Set), Nova Science Publishers, Inc., Hauppauge, NY, 2018, pp. 235–272.
[3] A. Sun, Lysosomal storage disease overview, Ann. Transl. Med. 6 (24) (2018) 476.
[4] K. Sawamoto, et al., Therapeutic options for mucopolysaccharidoses: current and emerging treatments, Drugs 79 (10) (2019) 1103–1134.
[5] C.J. Hendriksz, et al., Efficacy and safety of enzyme replacement therapy with BMN 110 (elosulfase alfa) for Morquio A syndrome (mucopolysaccharidosis IVA): a phase 3 randomised placebo-controlled study, J. Inherit. Metab. Dis. 37 (6) (2014) 979–990.
[6] K. Sawamoto, et al., Current therapies for Morquio A syndrome and their clinical outcomes, Expert Opin Orphan Drugs 4 (9) (2016) 941–951.
[7] M. Sanford, J.H. Lo, Elosulfase alfa: first global approval, Drugs 74 (6) (2014) 713–718.
[8] S. Tomatsu, et al., Enzyme replacement therapy for treating mucopolysaccharidosis type IVA (Morquio A syndrome): effect and limitations, Expert Opin. Orphan Drugs 3 (11) (2015) 1279–1290.
[9] Y. Puckett, H. Mulinder, A.M. Montaño, Enzyme replacement therapy with elosulfase alfa for mucopolysaccharidosis IVA (Morquio A syndrome): milestones and challenges, Expert Opin Orphan Drugs 5 (9) (2017) 741–752.
[10] A.J. Espejo-Mojica, et al., Human recombinant lysosomal enzymes produced in microorganisms, Mol. Genet. Metabol. 116 (1–2) (2015) 13–23.
[11] H. Du, et al., Enzyme therapy for lysosomal acid lipase deficiency in the mouse, Hum. Mol. Genet. 10 (16) (2001) 1639–1648.
[12] H. Du, et al., The role of mannosylated enzyme and the mannose receptor in enzyme replacement therapy, Am. J. Hum. Genet. 77 (6) (2005) 1061–1074.
[13] N. Pimentel, et al., Production and characterization of a human lysosomal recombinant iduronate-2-sulfatase produced in Pichia pastoris, Biotechnol. Appl. Biochem. 65 (5) (2018) 655–664.
[14] A. Rodriguez-Lopez, et al., Recombinant human N-acetylgalactosamine-6-sulfate sulfatase (GALNS) produced in the methylotrophic yeast Pichia pastoris, Sci. Rep. 6 (2016) 29329.
[15] A. Rodriguez-Lopez, et al., Characterization of human recombinant N-acetylgalactosamine-6-sulfate sulfatase produced in Pichia pastoris as potential enzyme for mucopolysaccharidosis IVA treatment, J. Pharmaceut. Sci. 108 (8) (2019) 2534–2541.
[16] A.J. Espejo-Mojica, et al., Characterization of recombinant human lysosomal beta-hexosaminidases produced in the methylotrophic yeast Pichia pastoris, Univ. Sci. 21 (2016) 195–217.
[17] A.J. Espejo-Mojica, et al., Human recombinant lysosomal beta-Hexosaminidases produced in Pichia pastoris efficiently reduced lipid accumulation in Tay-Sachs fibroblasts, Am. J. Med. Genet. Part C, Seminars in medical genetics 184 (4) (2020) 885–895.
[18] B. Laukens, C. De Visscher, N. Callewaert, Engineering yeast for producing human glycoproteins: where are we now? Future Microbiol. 10 (1) (2015) 21–34.
[19] L. Sanchez-Garcia, et al., Recombinant pharmaceuticals from microbial cells: a 2015 update, Microb. Cell Factories 15 (2016) 33.
[20] A. Eskandari, et al., Essential factors, advanced strategies, challenges, and approaches involved for efficient expression of recombinant proteins in Escherichia coli, Arch. Microbiol. 206 (4) (2024) 152.
[21] I. Incir, O. Kaplan, Escherichia coli as a versatile cell factory: advances and challenges in recombinant protein production, Protein Expr. Purif. 219 (2024) 106463.
[22] J.L. Baker, E. Celik, M.P. DeLisa, Expanding the glycoengineering toolbox: the rise of bacterial N-linked protein glycosylation, Trends Biotechnol. 31 (5) (2013) 313–323.
[23] D.C. Anyaogu, U.H. Mortensen, Manipulating the glycosylation pathway in bacterial and lower eukaryotes for production of therapeutic proteins, Curr. Opin. Biotechnol. 36 (2015) 122–128.
[24] H. Nothaft, C.M. Szymanski, Protein glycosylation in bacteria: sweeter than ever, Nat. Rev. Microbiol. 8 (11) (2010) 765–778.
[25] C.M. Szymanski, et al., Evidence for a system of general protein glycosylation in Campylobacter jejuni, Mol. Microbiol. 32 (5) (1999) 1022–1030.
[26] M. Kowarik, et al., N-linked glycosylation of folded proteins by the bacterial oligosaccharyltransferase, Science 314 (5802) (2006) 1148–1150.
[27] C. Lizak, et al., X-ray structure of a bacterial oligosaccharyltransferase, Nature 474 (7351) (2011) 350–355.
[28] M. Wacker, et al., N-linked glycosylation in Campylobacter jejuni and its functional transfer into E-coli, Science 298 (5599) (2002) 1790–1793.
[29] J.D. Valderrama-Rincon, et al., An engineered eukaryotic protein glycosylation pathway in Escherichia coli, Nat. Chem. Biol. 8 (5) (2012) 434–436.
[30] M.F. Feldman, et al., Engineering N-linked protein glycosylation with diverse O antigen lipopolysaccharide structures in Escherichia coli, Proc. Natl. Acad. Sci. U. S. A. 102 (8) (2005) 3016–3021.
[31] C.J. Glasscock, et al., A flow cytometric approach to engineering Escherichia coli for improved eukaryotic protein glycosylation, Metab. Eng. 47 (2018) 488–495.
[32] A. Rodriguez, et al., Enzyme replacement therapy for Morquio A: an active recombinant N-acetylgalactosamine-6-sulfate sulfatase produced in Escherichia coli BL21, J. Ind. Microbiol. Biotechnol. 37 (11) (2010) 1193–1201.
[33] A. Mosquera, et al., Characterization of a recombinant N-acetylgalactosamine-6-sulfate sulfatase produced in E. coli for enzyme replacement therapy of Morquio A disease, Process Biochem. 47 (2012) 2097–2102.
[34] A. Hernandez, et al., Effect of culture conditions and signal peptide on production of human recombinant N-acetylgalactosamine-6-sulfate sulfatase in Escherichia coli BL21, J. Microbiol. Biotechnol. 23 (5) (2013) 689–698.
[35] L.H. Reyes, et al., Improvement in the production of the human recombinant enzyme N-acetylgalactosamine-6-sulfatase (rhGALNS) in Escherichia coli using synthetic biology approaches, Sci. Rep. 7 (1) (2017) 5844–5858.
[36] A. Mosquera, et al., Characterization of a recombinant N-acetylgalactosamine-6-sulfate sulfatase produced in E. coli for enzyme replacement therapy of Morquio A disease, Process Biochem. 47 (12) (2012) 2097–2102.

[37] F.M. Ausubel, et al., in: J.W. Sons (Ed.), Short Protocols in Molecular Biology: A Compendium of Methods from Current Protocols in Molecular Biology, fourth ed., 1999.
[38] O.P. van Diggelen, et al., A fluorimetric enzyme assay for the diagnosis of Morquio disease type A (MPS IV A), Clin. Chim. Acta 187 (2) (1990) 131–139.
[39] S. Tomatsu, et al., Characterization and pharmacokinetic study of recombinant human N-acetylgalactosamine-6-sulfate sulfatase, Mol. Genet. Metabol. 91 (1) (2007) 69–78.
[40] C.A. Schneider, W.S. Rasband, K.W. Eliceiri, NIH Image to ImageJ: 25 years of image analysis, Nat. Methods 9 (7) (2012) 671–675.
[41] F. Kubaski, et al., Newborn screening for mucopolysaccharidoses: a pilot study of measurement of glycosaminoglycans by tandem mass spectrometry, J. Inherit. Metab. Dis. 40 (1) (2017) 151–158.
[42] F. Kubaski, et al., Glycosaminoglycan levels in dried blood spots of patients with mucopolysaccharidoses and mucolipidoses, Mol. Genet. Metabol. 120 (3) (2017) 247–254.
[43] J.M. Perchiacca, et al., Structure-based design of conformation- and sequence-specific antibodies against amyloid beta, Proc. Natl. Acad. Sci. U.S.A. 109 (1) (2012) 84–89.
[44] M. Dvorak-Ewell, et al., Enzyme replacement in a human model of mucopolysaccharidosis IVA In-vitro and its biodistribution in the cartilage of wild type mice, PLoS One 5 (8) (2010) e12194.
[45] P. Bojarova, S.J. Williams, Sulfotransferases, sulfatases and formylglycine-generating enzymes: a sulfation fascination, Curr. Opin. Chem. Biol. 12 (5) (2008) 573–581.
[46] C. Alméciga-Díaz, et al., Adeno-associated virus gene transfer on Morquio A: effect of promoters and sulfatase-modifying Factor 1, FEBS J. 277 (17) (2010) 3608–3619.
[47] A. Fraldi, et al., SUMF1 enhances sulfatase activities in vivo in five sulfatase deficiencies, Biochem. J. 403 (2) (2007) 305–312.
[48] S. Tomatsu, et al., Enzyme replacement therapy in a murine model of Morquio A syndrome, Hum. Mol. Genet. 17 (6) (2008) 815–824.
[49] Q.H. Zhou, et al., Brain-penetrating IgG-iduronate 2-sulfatase fusion protein for the mouse, Drug Metab. Dispos. 40 (2) (2012) 329–335.
[50] C.J. Almeciga-Diaz, et al., Anaerobic sulfatase maturase AslB from Escherichia coli activates human recombinant iduronate-2-sulfate sulfatase (IDS) and N-acetylgalactosamine-6-sulfate sulfatase (GALNS), Gene 634 (2017) 53–61.
[51] G.L. Rosano, E.A. Ceccarelli, Recombinant protein expression in Escherichia coli: advances and challenges, Front. Microbiol. 5 (172) (2014) 1–7.
[52] J.E. Peters, T.E. Thate, N.L. Craig, Definition of the Escherichia coli MC4100 genome by use of a DNA array, J. Bacteriol. 185 (6) (2003) 2017–2021.
[53] H.P. Sorensen, K.K. Mortensen, Advanced genetic strategies for recombinant protein expression in Escherichia coli, J. Biotechnol. 115 (2) (2005) 113–128.
[54] F. Baneyx, M. Mujacic, Recombinant protein folding and misfolding in Escherichia coli, Nat. Biotechnol. 22 (11) (2004) 1399–1408.
[55] J. Bielicki, J.J. Hopwood, Human liver N-acetylgalactosamine 6-sulphatase. Purification and characterization, Biochem. J. 279 (Pt 2) (1991) 515–520.
[56] M. Masue, et al., N-acetylgalactosamine-6-sulfate sulfatase in human placenta: purification and characteristics, J. Biochem. 110 (6) (1991) 965–970.
[57] S. Tomatsu, et al., Characterization and pharmacokinetic study of recombinant human N-acetylgalactosamine-6-sulfate sulfatase, Mol. Genet. Metabol. 91 (1) (2007) 69–78.
[58] S. Olarte-Avellaneda, et al., Computational analysis of human N-acetylgalactosamine-6-sulfate sulfatase enzyme: an update in genotype-phenotype correlation for Morquio A, Mol. Biol. Rep. 41 (11) (2014) 7073–7088.
[59] Y. Rivera-Colon, et al., The structure of human GALNS reveals the molecular basis for mucopolysaccharidosis IV A, J. Mol. Biol. 423 (5) (2012) 736–751.
[60] M. Kowarik, et al., Definition of the bacterial N-glycosylation site consensus sequence, EMBO J. 25 (9) (2006) 1957–1966.
[61] J. Glossl, W. Truppe, H. Kresse, Purification and properties of N-acetylgalactosamine 6-sulphate sulphatase from human placenta, Biochem. J. 181 (1) (1979) 37–46.
[62] A. Helenius, M. Aebi, Intracellular functions of N-linked glycans, Science 291 (5512) (2001) 2364–2369.
[63] R.J. Sola, K. Griebenow, Effects of glycosylation on the stability of protein pharmaceuticals, J. Pharmaceut. Sci. 98 (4) (2009) 1223–1245.
[64] H. Zhao, et al., Prenatal diagnosis of Morquio disease type A using a simple fluorometric enzyme assay, Prenat. Diagn. 10 (2) (1990) 85–91.
[65] J.W. Jung, et al., Production of recombinant human acid alpha-glucosidase with high-mannose glycans in gnt1 rice for the treatment of Pompe disease, J. Biotechnol. 249 (2017) 42–50.
[66] G.A. Grabowski, M. Golembo, Y. Shaaltiel, Taliglucerase alfa: an enzyme replacement therapy using plant cell expression technology, Mol. Genet. Metabol. 112 (1) (2014) 1–8.
[67] J.S. Shen, et al., Mannose receptor-mediated delivery of moss-made alpha-galactosidase A efficiently corrects enzyme deficiency in Fabry mice, J. Inherit. Metab. Dis. 39 (2) (2016) 293–303.
[68] H.J. Jurgensen, et al., Complex determinants in specific members of the mannose receptor family govern collagen endocytosis, J. Biol. Chem. 289 (11) (2014) 7935–7947.
[69] Y. Chiba, et al., Production in yeast of alpha-galactosidase A, a lysosomal enzyme applicable to enzyme replacement therapy for Fabry disease, Glycobiology 12 (12) (2002) 821–828.
[70] Y. Shaaltiel, et al., Production of glucocerebrosidase with terminal mannose glycans for enzyme replacement therapy of Gaucher's disease using a plant cell system, Plant Biotechnol. J. 5 (5) (2007) 579–590.
[71] P. Paracuellos, et al., Insights into collagen uptake by C-type mannose receptors from the crystal structure of Endo180 domains 1-4, Structure 23 (11) (2015) 2133–2142.
[72] J. Boskovic, et al., Structural model for the mannose receptor family uncovered by electron microscopy of Endo180 and the mannose receptor, J. Biol. Chem. 281 (13) (2006) 8780–8787.
[73] O. Llorca, Extended and bent conformations of the mannose receptor family, Cell. Mol. Life Sci. : CM 65 (9) (2008) 1302–1310.
[74] S. Markmann, et al., Lrp1/LDL receptor play critical roles in mannose 6-phosphate-independent lysosomal enzyme targeting, Traffic 16 (7) (2015) 743–759.
[75] T. Shimada, et al., Di-sulfated keratan sulfate as a novel biomarker for mucopolysaccharidosis II, IVA, and IVB, JIMD Rep 21 (2015) 1–13.
[76] S. Khan, et al., Mucopolysaccharidosis IVA and glycosaminoglycans, Mol. Genet. Metabol. 120 (1–2) (2017) 78–95.
[77] S. Tomatsu, et al., Mouse model of N-acetylgalactosamine-6-sulfate sulfatase deficiency (Galns-/-) produced by targeted disruption of the gene defective in Morquio A disease, Hum. Mol. Genet. 12 (24) (2003) 3349–3358.
[78] S. Tomatsu, et al., Development of MPS IVA mouse (Galnstm(hC79S.mC76S)slu) tolerant to human N-acetylgalactosamine-6-sulfate sulfatase, Hum. Mol. Genet. 14 (2005) 3321–3335.
[79] S. Tomatsu, et al., Murine model (Galns(tm(C76S)slu)) of MPS IVA with missense mutation at the active site cysteine conserved among sulfatase proteins, Mol. Genet. Metabol. 91 (3) (2007) 251–258.
[80] F. Kubaski, et al., Glycosaminoglycans detection methods: applications of mass spectrometry, Mol. Genet. Metabol. 120 (1–2) (2017) 67–77.
[81] W. Sun, W. Zheng, A. Simeonov, Drug discovery and development for rare genetic disorders, Am. J. Med. Genet. (2017).